JOURNAL OF MATERIALS SCIENCE 33 (1998) 1783–1787

# Structural properties of $Pb(Zr_{0.53}Ti_{0.47})O_3$/$YBa_2Cu_3O_{7-\delta}$ heterostructures on $SrTiO_3$ substrates

C. R. LI*, J. H. JIANG‡, W. WU, D. Y. DAI§, A. J. ZHU, H. T. YANG‡, H. J. TAO‡, C. Y. WANG, B. R. ZHAO‡, L. LI‡ and Z. H. MAI
*Institute of Physics and Centre for Condensed Matter Physics,*
*‡National Laboratory for Superconductivity,*
*§National Microgravity Laboratory, Chinese Academy of Sciences, Beijing 100080, People's Republic of China.*
*E-mail: cuizhai@aphy02.iphy.ac.cn*

The structures of ferroelectric $Pb(Zr_{0.53}Ti_{0.47})O_3$ and high-$T_c$ $YBa_2Cu_3O_{7-\delta}$ superconductor integrated films on (001) $SrTiO_3$ substrate prepared by the r.f./d.c. magnetron sputtering method have been studied by X-ray grazing incidence reflectivity, diffuse scattering and high-resolution X-ray diffraction methods combined with atomic force microscopy (AFM) and SEM techniques. The results of high-resolution X-ray diffraction show that the quality of $Pb(Zr_{0.53}Ti_{0.47})O_3$ improved as the thickness increased. On the other hand, the crystalline quality of $YBa_2Cu_3O_{7-\delta}$ deteriorated and the superconducting transition temperature, $T_c$, decreased as the thickness of $Pb(Zr_{0.53}Ti_{0.47})O_3$ increased. The strain state was similar for different thickness samples and the lattice mismatch strain in the $Pb(Zr_{0.53}Ti_{0.47})O_3$ layer was almost totally relaxed. The root mean square (r.m.s.) roughness at $Pb(Zr_{0.53}Ti_{0.47})O_3/YBa_2Cu_3O_{7-\delta}$ interface was determined to be about $1.7 \pm 0.3$ nm by X-ray specular reflectivity. The r.m.s. roughness at the surface of $Pb(Zr_{0.53}Ti_{0.47})O_3/YBa_2Cu_3O_{7-\delta}$ bilayer samples was about 1.5 to $2.0 \pm 0.3$ nm which was larger than that of $YBa_2Cu_3O_{7-\delta}$ single-layer sample measured by both X-ray specular reflectivity and AFM methods. The results from AFM and SEM show that the morphological characteristics of the $Pb(Zr_{0.53}Ti_{0.47})O_3$ layer surface were large grains covering about 10% in area distributed on a fine-grained matrix.


## 1. Introduction

Ferroelectric and high-$T_c$ superconductor heterostructures have attracted remarkable attention recently [1–3], because of their physical properties and device applications. Ferroelectric films have large potential application in solid-state devices such as microactuators, non-volatile memories, infrared detectors, etc., based upon their dielectric, piezoelectric, pyroelectric and ferroelectric-optic effects, etc. The $Pb(Zr_xTi_{1-x})O_3$ (PZT) thin film is a most interesting material in its applications in the non-volatile ferroelectric random access memory (FRAM) [4]. The usage of high-$T_c$ $YBa_2Cu_3O_{7-\delta}$ film (YBCO) as an electrode instead of using normal metals such as gold or platinum can improve the fatigue properties of FRAMs [5], because the crystalline quality of the PZT layer and the interface between the PZT and the electrode are improved by the YBCO layer, in addition to its good metallic behaviour in the normal state.

It is known that for PZT/YBCO heterostructures, the dielectric loss is abruptly reduced when the temperature is reduced below $T_c$ [6]. This phenomenon is believed to be related to the interface structure of PZT/YBCO. As is well known, the interface structure between PZT and electrode is a crucial factor for controlling the fatigue behaviour and other physical properties. Therefore, it is very important to investigate the PZT/YBCO interface as well as other structure properties. The interfacial structures used to be analysed by Auger electron spectroscopy (AES) [7, 8] and transmission electron microscopy (TEM) [3], etc. The crystalline quality was usually estimated from X-ray powder diffraction profiles. However, there is a disadvantage in using these methods as they are either destructive or the accuracy is relatively low. In this paper, the surface and interface properties of PZT/YBCO bilayer samples with different PZT layer thicknesses, were investigated by grazing X-ray incidence reflectivity and diffuse scattering. The crystalline quality of PZT and YBCO layers were studied by high-resolution X-ray diffraction. The morphology of the surface was observed by atomic

*Author to whom all correspondence should be addressed.

force microscopy (AFM) and scanning electron microscopy (SEM).

## 2. Experimental procedure

The samples were grown by the r.f./d.c. magnetron sputtering method. The detailed deposition procedure and parameters have been published elsewhere [3, 9]. The target of PZT was sintered from a pressed-disc of a mixture of PbO, $ZrO_2$ and $TiO_2$ powders. The YBCO target was sintered stoichiometric YBCO. The YBCO layer was deposited by d.c. magnetron sputtering at a temperature of 680 °C. The PZT layer was then deposited by r.f. magnetron sputtering at a temperature of 630°C. After deposition, the sample was annealed at 480°C under about 1 atm oxygen gas for 30 min then cooled down to room temperature. In order to investigate the crystalline quality of the PZT and its influence on the YBCO, samples with different PZT layer thicknesses were prepared. The deposition times for the various samples are listed in Table I.

The superconductivity transition temperature, $T_c$, was measured by a.c. susceptibility. The resulting values of $T_c$ are shown in Table I. The surface morphologies of YBCO and PZT were observed by AFM and SEM. X-ray reflection and high-resolution diffraction data were collected on a Phillips X'Pert MRD X-ray diffractometer with CuK$\alpha$ radiation. During the reflection experiments, the thin-film attachments were used. The Soller slits and graphite analyser were set at the front of the detector. The acceptance angle of the detector was about 0.058°. The divergency of the incident beam was confined to be about 0.03° by a slit. Grazing incidence specular, off-specular reflectivities, and transverse scans, were performed. During the high-resolution X-ray diffraction, the high-resolution monochromator with a Ge 2 2 0 (+, −, −, +) diffraction arrangement was used. X-ray double-crystal diffraction rocking curves were recorded close to $SrTiO_3$ (0 0 2) symmetrical and (1 0 3) asymmetrical diffractions. In order to determine accurately the strain state of the layers, rocking curves were measured at azimuth angles of 0° and 180° to the surface normal. The misorientation between the substrate and layer (0 0 1) crystalline direction and the lattice parameter perpendicular to the (0 0 1) lattice plane were determined by recording the (0 0 2) symmetrical diffractions. The grazing incidence and grazing exit (1 0 3) asymmetrical diffractions were used in order to determine the lattice parameter parallel to (0 0 1) lattice plane.

TABLE I The deposition time of YBCO and PZT layers and the superconducting temperature of different samples

| Sample | Deposition time (min) | | $T_c$ (K) |
|---|---|---|---|
| | YBCO | PZT | |
| A | 40 | – | 88 |
| B | 40 | 10 | 85 |
| C | 40 | 20 | 84 |
| D | 40 | 30 | 83 |

## 3. Results and discussion

### 3.1. X-ray grazing incident specular reflectivity measurements

The X-ray specular reflectivity spectra are shown in Fig. 1 for samples A, B and C. The theoretical profiles were calculated using matrix formulation [10] based upon Fresnel's law in classical optics. For a real interface, a roughness parameter, $\sigma$, representing the root mean square (r.m.s.) is introduced, and deviations of interfacial height from an ideal planar boundary are assumed to follow a normal Gaussian distribution. It is clear from Fig. 1 that there were distinct interference fringes in reflectivity spectra of the samples, which corresponded to thickness of layers and interface

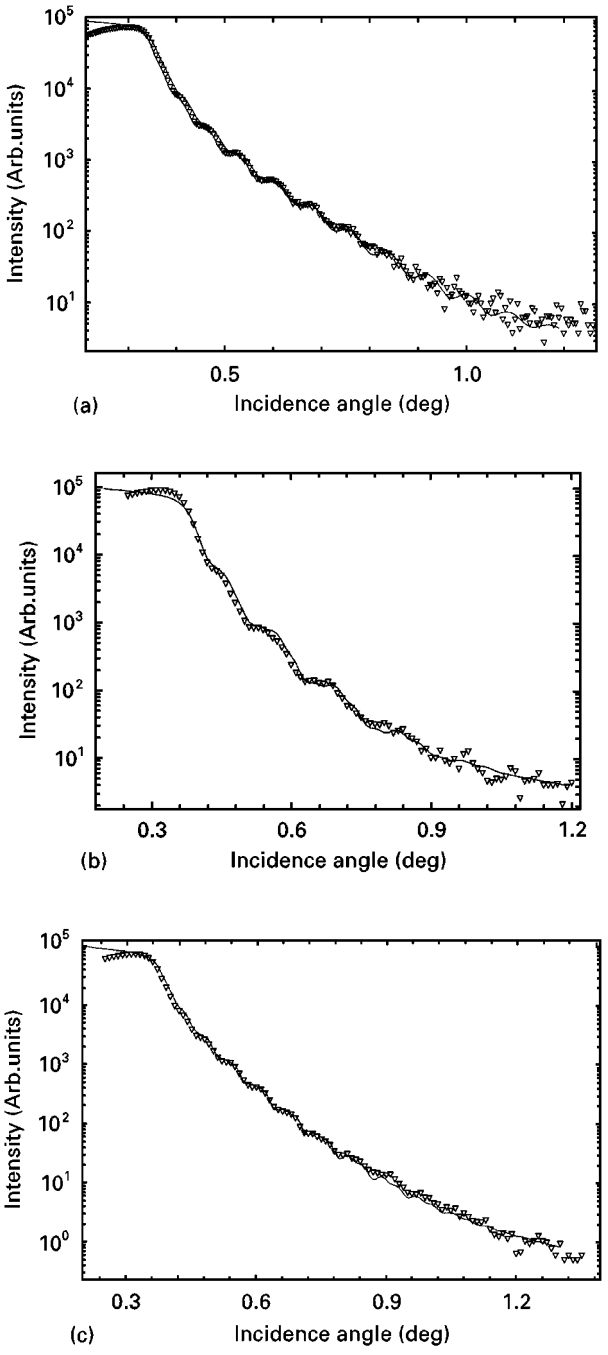


*Figure 1* X-ray specular reflectivity of (a) sample A, (b) sample B, (c) sample C. (∇) experiment; (——) simulation; The best fit parameters to the experimental profiles for the samples are listed in Table II.

TABLE II The simulation structure parameters of the samples

| Sample | $t_{YBCO}$ (nm) | $t_{PZT}$ (nm) | $\sigma_{STO/YBCO}$ (nm) | $\sigma_{YBCO/PZT}$ (nm) | $\sigma_{PZT}$ (nm) |
|---|---|---|---|---|---|
| A | 49.6 | | 1.0 | 1.15 | |
| B | 50 | 26.5 | 1.2 | 1.4 | 1.8 |
| C | 50 | 51 | 1.4 | 1.6 | 1.6 |
| D | 50 | 80 | | | |

roughness. Because sample A contained only one single YBCO layer, the determination of structure parameters, such as layer thickness, surface and interface roughness was quite direct and accurate through the simulation of the experimental profile. As is well known, the fringe contrast depends on the electron density difference between the two layers across an interface. Because the electron density difference between PZT and YBCO is much larger than that between YBCO and $SrTiO_3$ substrate, the fringe contrast was dominated by the PZT layer in the bilayer samples. It was reasonable to use the same YBCO layer thickness while calculating the reflectivity spectra of bilayer samples B and C, because the YBCO deposition time and other conditions were the same for all the samples concerned. The structure parameters obtained from the best fit of the experimental reflectivity spectra are listed in Table II. It can be seen from Table II that the interface roughness, $\sigma_{YBCO/PZT}$, of bilayer samples B and C is larger than the surface roughness of the single-layer sample A. The interface roughness, $\sigma_{YBCO/PZT}$, increased slightly as the PZT layer thickness increased. The surface may not have been physically flat in sample D. Therefore, no fringes could be seen in the reflectivity profile, leading to the determination of inaccurate layer structure parameters for sample D.

## 3.2. Surface morphology

The surface morphologies were observed by SEM and AFM. Typical surface characteristics of the YBCO single layer consisted of some large grains, which had a clear geometrical face and their surfaces were relatively smooth and flat, distributed on a relatively smooth base. The large grains were up to several hundred nanometres in size, while their total area was only about 10% of the whole view. For the surface of the PZT/YBCO bilayer, there were fine PZT grains distributed homogeneously on both the large grains and other areas of the surface of YBCO. Fig. 2 shows the AFM surface morphologies of a relative flat area of the samples. The size of the PZT grains increased as the thickness of PZT increased. The PZT grain size of sample C was about twice that of sample B.

The height distribution of the large grains on both the single layer and bilayer samples ranged from several, to hundreds of nanometres as measured from the AFM line profiles. The maximum height fluctuations in other areas of the YBCO single layer and for the PZT/YBCO bilayer were about 2.4 and 8 nm, respectively. The area scan shows that the surface r.m.s. roughness was 1.74 and 1.48 nm for sample B (scan area about $1 \times 1\ \mu m^2$) and C, respectively, which agrees well with the X-ray reflectivity results shown in Table II. The slight difference of surface roughness from AFM and X-ray reflectivity measurements could be due to the fact that the detected area of AFM was much smaller than that detected by the X-ray reflectivity method.

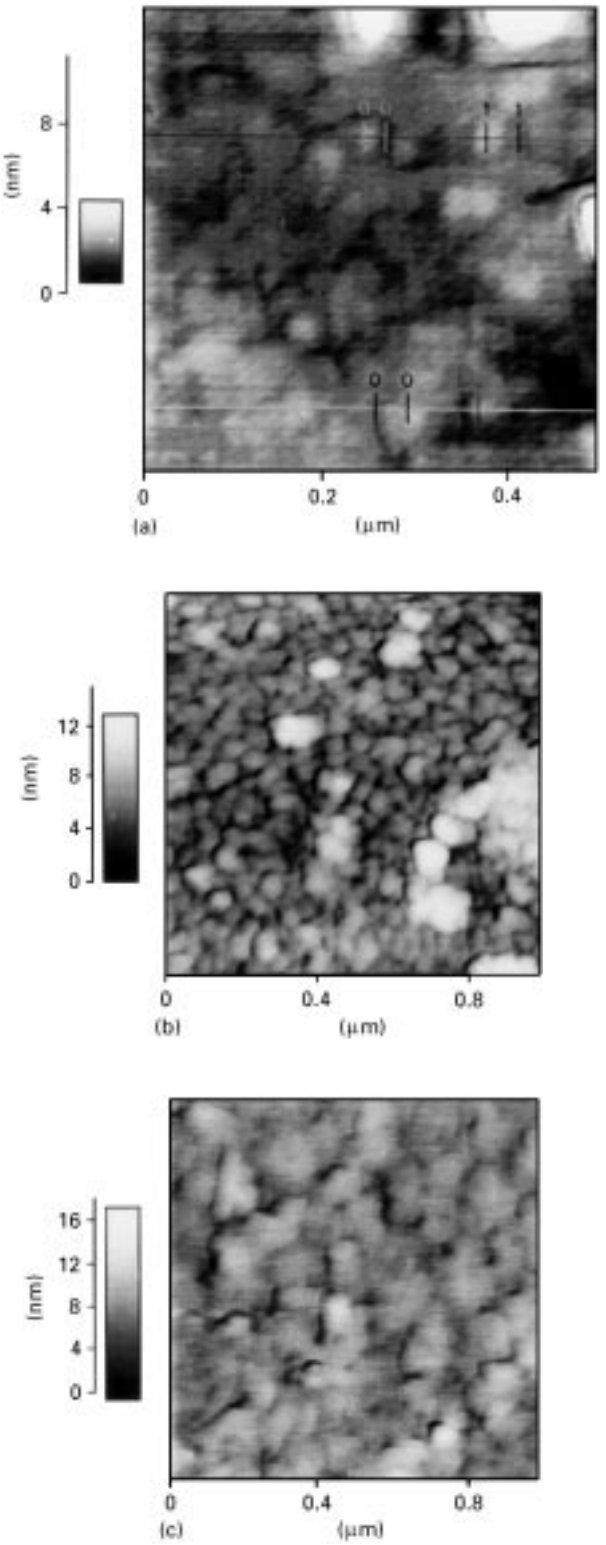


*Figure 2* AFM surface morphology of (a) sample A, (b) sample B, (c) sample C.

### 3.3. High-resolution X-ray diffraction

The double-crystal diffraction rocking curves of (0 0 2) symmetrical and (1 0 3) grazing incidence and grazing exit asymmetrical diffractions for sample C are shown in Fig. 3a and b, respectively. From Fig. 3a, one can deduce that there is a misorientation angle in the [0 0 1] direction between the layers and substrate. The misorientation angles, δ, for YBCO and PZT were about 0.09° and 0.06°, respectively. It is evident that for the (1 0 3) grazing incidence and exit geometry the angular distance between the PZT peak and the $SrTiO_3$ substrate peaks were close to each other, being about 2.09°. This meant that the PZT lattice plane of (1 0 3) was parallel to that of the $SrTiO_3$ substrate. Therefore, the residual strain in the PZT layer, caused by lattice mismatch between the layer and the substrate, was very small and the strain was almost totally relaxed. The angular distance of the YBCO (0 0 5) and the PZT (0 0 2) peaks to the substrate peak, the full-widths at half-maximum (FWHM) of the (0 0 2) diffraction peaks and the misorientation angle of the layer to the substrate are listed in Table III. We investigated the YBCO (0 0 5) diffraction peak, because it is well separated from the (0 0 2) diffraction peak of $SrTiO_3$, while the YBCO (0 0 6) diffraction peak is hard to isolate from the substrate (0 0 2) diffraction peak. The relative angular positions and FWHM of the layer peaks were determined by fitting the shape of the layer peak with a Gaussian distribution function. We found that there was little difference in the relative angular distance between the layer peaks and the substrate peak for all samples. Because the angular distance of YBCO (0 0 5) to $SrTiO_3$ (0 0 2) for bilayer samples is almost the same as that of the YBCO single-layer sample, it was reasonable to assume that the strain state of YBCO was similar whether or not PZT was present. The angular distance between the PZT (0 0 2) and $SrTiO_3$ (0 0 2) for the samples with different layer thickness shows that the lattice mismatch strain relaxation was nearly the same and the layer was almost totally relaxed.

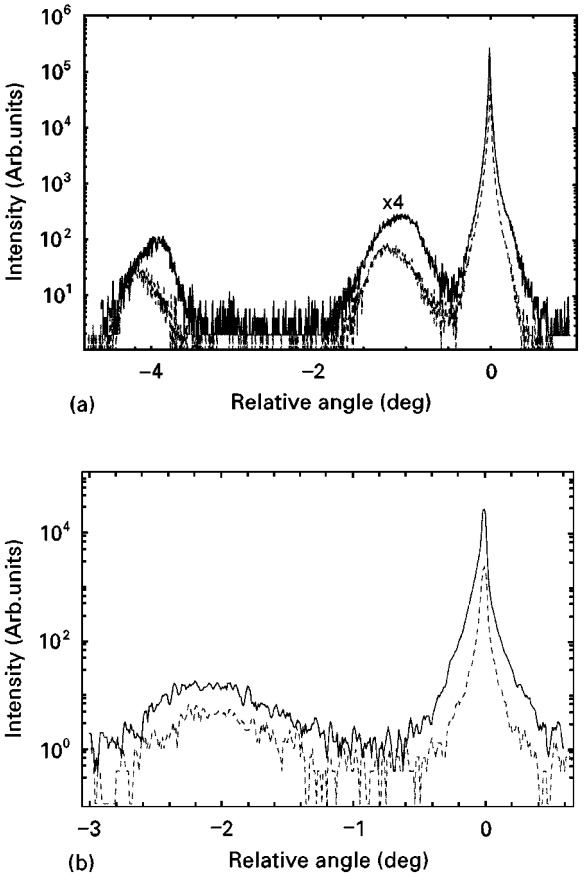


*Figure 3* X-ray double crystal diffraction rocking curves of sample C. (a) (0 0 2) symmetrical diffraction, with measurement along the azimuth angle surface normal, ϕ, of (——) 0° and ( – – – ) 180°. (b) (1 0 3) asymmetrical diffraction; (——) the grazing incident and (---) exit geometry.

As is well known, the FWHM of the diffraction peak in X-ray double crystal rocking curve analysis can be used to evaluate qualitatively the crystalline quality. From Table III, it can be seen that the FWHM of the PZT (0 0 2) peak became smaller, as its thickness increased. This meant that the crystalline quality of PZT improved with increasing thickness. On the other hand, the FWHM of the YBCO (0 0 5) diffraction peak became larger as the depositing thickness of PZT increased. This implies that the deposition of PZT would degrade the crystalline quality of YBCO. This result differs from the earlier work by Ramesh *et al.* [11] in $Pb(Zr_{0.2}Ti_{0.8})\ O_3$/YBCO integrated films grown by a pulsed-laser deposition method, where the deposition of PZT did not degrade the crystalline quality of YBCO. The superconductivity transition temperature measured by a.c. susceptibility also displayed this degrading effect. The reason was probably due to the difficulty of getting oxygen into the YBCO thin film during the annealing process after the deposition of PZT. The thicker the PZT layer, the harder it is for the YBCO to obtain oxygen. The X-ray reflectivity results also showed that the deposition of PZT will roughen the YBCO/PZT interface. The relatively large FWHM value of the YBCO single layer in sample A may have been due to its long exposure time in air.

TABLE III The angular distance of the YBCO layer (0 0 5) and the PZT layer (0 0 2) diffraction peaks to the $SrTiO_3$ (0 0 2) substrate peak, FWHM of layer peaks and misorientation of the layers to the substrate

| Sample | $\Delta\theta_{YBCO\text{-}STO}$ (deg) | $\Delta\theta_{PZT\text{-}STO}$ (deg) | $FWHM_{YBCO(0\,0\,5)}$ (deg) | $FWHM_{PZT(0\,0\,2)}$ (deg) | $\delta_{YBCO}$ (deg) | $\delta_{PZT}$ (deg) |
|---|---|---|---|---|---|---|
| A | 4.030 | | 0.385 | | 0 | |
| B | 4.032 | 1.124 | 0.328 | 0.550 | 0.045 | 0.022 |
| C | 4.030 | 1.120 | 0.385 | 0.483 | 0.09 | 0.06 |
| D | 4.073 | 1.143 | 0.515 | 0.445 | 0.001 | 0.01 |

## 4. Conclusion

A heterostructure of PZT/YBCO grown by r.f./d.c. magnetron sputtering was investigated by X-ray grazing incidence reflectivity, X-ray high-resolution diffraction, AFM and SEM. The r.m.s. roughness at PZT/YBCO bilayer sample surface was found to be about 1.6–1.8 $\pm$ 0.2 nm, which was larger than that at the YBCO single surface, about 1.15 $\pm$ 0.2 nm. The interfacial roughness at PZT/YBCO was about 1.6 $\pm$ 0.4 nm. The crystalline quality of the PZT layer improved as its thickness increased. However, depositing a thick PZT layer degraded the crystalline quality of YBCO and roughened the PZT/YBCO interface. The mismatch strain in the PZT layer was almost totally relaxed.


## Acknowledgements

Financial support from National Nature Sciences Foundation of China and the Chinese National Centre for Research and Development on Superconductivity is acknowledged.


## References


1. C. H. AHN, J.-M. TRISCONE, N. ARCHIBALD, M. DECROUX, R. H. HAMMOND, T. H. GEBALLE, Ø. FISCHER and M. R. BEASLEY, *Science* **269** (1995) 373.
2. G. BJ MANDER, A. M. GRISHIN, B. M. MOON, J. LEE and K. V. RAO, *Appl. Phys. Lett.* **64** (1994) 3646.
3. L. X. CAO, Y. XU, B. R. ZHAO, L. P. GUO, J. Z. LIU, B. XU, F. WU, L. LI, Z. X. ZHAO, A. J. ZHU, Z. H. MAI, J. H. ZHAO, Y. F. FU and X. J. LI, *Supercond. Sci. Technol.* **9** (1996) 310.
4. G. H. HAERTILING, *J. Vac. Sci. Technol.* **9** (1991) 414.
5. R. RAMESH, W. K. CHAN, B. WILKENS, H. GILCHRIST, T. SANDS, J. M. TARASCON, D. K. FORK, J. LEE and A. SAFARI, *Appl.. Phys. Lett.* **61** (1992), 1537.
6. H. LIN, N. J. WU, K. XIE, X. Y. LI and A. IGNATIEV, *Integr. Ferroelect.* **5** (1994) 197.
7. L. X. CAO, Y. XU, B. R. ZHAO, T. YANG, Y. ZHU, D. F. ZHANG, J. H. ZHAO, Y. F. FU, X. J. LI, B. XU, Y. Z. ZHANG, F. WU, B. YIN, S. Q. GUO, J. W. LI, S. L. JIA, J. H. JIANG and L. LI, *Physica C* **266** (1996) 143.
8. N. J. WU, A. IGNATIV, A.-W. MESARWI, L. HE, K. XIE and H.-D. SHIH, *Jpn. J. Appl. Phys.* **32** (1993) 5019.
9. L. X. CAO, Y. XU, B. R. ZHAO, B. XU, F. WU, L. LI and Z. X. ZHAO, *Chin. Sci. Bull.* **41** (1996) 372.
10. Z. H. MING, A. KROL, Y. L. SOO, Y. H. KAO, J. S. PARK and K. L. WANG, *Phys. Rev.* **B47** (1993) 16373.
11. R. RAMESH, A. INAM, W. K. CHAN, F. TILLEROT, B. WILKENS, C. C. CHANG, T. SANDS, S. M. TARASON and V. G. KERAMIDAS, *Appl. Phys. Lett.* **59** (1991) 3542.



*Received 18 March*
*and accepted 5 December 1997*